 CMES, vol.51, no.1, pp.73-92, 2009

The Chebyshev Tau Spectral Method for the Solution of the Linear Stability Equations for Rayleigh-Bénard Convection with Melting

Rubén Avila[1], **Eduardo Ramos**[2] **and S. N. Atluri** [3]

Abstract: A Chebyshev Tau numerical algorithm is presented to solve the perturbation equations that result from the linear stability analysis of the convective motion of a fluid layer that appears when an unconfined solid melts in the presence of gravity. The system of equations that describe the phenomenon constitute an eigenvalue problem whose accurate solution requires a robust method. We solve the equations with our method and briefly describe examples of the results. In the limit where the liquid-solid interface recedes at zero velocity the Rayleigh-Bénard solution is recovered. We show that the critical Rayleigh number Ra_c and the critical wave number a_c are monotonically decreasing functions of the rate of melting of the solid. We conclude that the parameters Ra_c and a_c are independent functions of the Prandtl number in the range $1 \leq Pr \leq 10,000$. We also show that as the Pr number is reduced, $Pr < 1$, the critical parameters are nonmonotonic functions of the rate of melting.

Keywords: Tau-Chebyshev method, spectral method, stability analysis, phase change, melting.

1 Introduction

The melting of a solid body heated from below under the influence of the Earth's gravity force may lead to the instability and natural convective motion of the growing liquid phase. The melting of the solid material results in time-dependent physical and geometrical conditions of the liquid phase, which in turn have a large influence on the stability and convective flow pattern selection. A fundamental understanding of the onset of convective motion and the resulting flow patterns in the

[1] Departamento de Termofluidos, Facultad de Ingeniería, Universidad Nacional Autónoma de México, Mexico D.F. C.P. 04510, ravila@servidor.unam.mx
[2] Centro de Investigación en Energía, Universidad Nacional Autónoma de México, AP. P. 34, 62580, Temixco Mor. México, erm@mazatl.cie.unam.mx
[3] Center for Aerospace Research & Education, University of California, Irvine

fluid layer may lead to an increase in the performance of devices used in a large field of engineering applications such as in material processing [Langlois (1985)] and thermal energy storage [Sparrow, Schmidt, and Ramsey (1978); Zhang, Su, Zhu, and Hu (2001)]. In core melt progression studies, in hypothetical severe accidents in nuclear reactors, it has been concluded that an understanding of the convective motion in the molten material is crucial for the implementation of severe accident management strategies [Asmolov, Ponomarev-Stepnoy, Strizhov, and Sehgal (2001)]. In nature, the stability conditions, and the onset of natural convection in the liquid phase, contribute to an increase in the rate of melting of ice in the Earth's polar regions and glaciers. Another important geophysical system that continuously undergoes melting is the shallower level of the Earth's mantle (partial melting of the mantle rocks) [Ribe (1985)]. It is well known that the solution of problems in science and engineering where a moving interface is present, must be addressed by using sophisticated numerical techniques, which are based either on methodologies that require a numerical grid (finite elements, control volumes, spectral elements, etc.) or on meshfree numerical algorithms (meshless local Petrov Galerkin methods or meshfree local radial basis function collocation methods); see for example [Atluri and Zhu (1998); Lin and Atluri (2001); Avila and Solorio (2009); Kosec and Šarler (2009)].

The first systematic study of the stability of a fluid layer heated from below, in the presence of body forces, was performed by Rayleigh in a classical paper [Rayleigh (1916)] aimed to identify the conditions that lead to the onset of fluid motion. Rayleigh considered an infinite fluid layer of constant height and his analysis was restricted to linear perturbations. He established a set of equations derived from the fundamental principles of mass, momentum and energy conservation, that constitute an eigenvalue problem and solved them with an essentially analytical method. Reviews of Rayleigh's theory and its numerous extensions and generalizations can be found in monographes such as for example [Chandrasekhar (1961); Koschmieder (1993) and Getling (1998)]. A great deal of knowledge on the problem is now available, but it is recognized that in most cases, the solution of the equations must be sought by using numerical techniques. The stability of a fluid layer generated by the melting of a solid and consequently confined in a region whose height is a function of time has been studied less. This problem presents features similar to those of the classical Stefan problem where the position of the liquid-solid interface is a part of the solution. In the literature, the problem has been addressed by using various degrees of approximation. [Sparrow, Lee, and Shamsundar (1976)] conducted a numerical investigation of the convective instability of a melt layer heated from below; in their analysis, the temporal variation of the velocity and temperature perturbations was neglected. By using a shooting technique to solve the stability equations, they found a nonmonotonic variation of the critical Rayleigh number with the Stefan number of the system. [Liu (2006); Liu (2008); Liu, Chang, and Chang (2008)] have described in detail, the general characteristics of the shooting numerical technique. [Hwang (2001) and Smith (1988)] considered that the liquid-solid interface moves with a constant velocity, however, this assumption is inconsistent with observations of [Boger and Westwater (1967)] and with the well known theory on the Stefan problem [Stefan (1891); Carlslaw and Jaeger (1959)]. [Kim, Lee, and Choi (2008)] considered essentially the same problem which is the subject of the present investigation, however they used an outward shooting scheme to solve a different version of the set of stability equations.

In this paper, we present the numerical solution of the stability equations for Rayleigh-Bénard convection in systems with melting from below. We have developed a robust and well founded numerical algorithm in which the velocity and temperature perturbations are approximated by using Chebyshev polynomials. This spectral numerical technique has been widely used to carry out linear stability analysis in thermal and fluid dynamics applications [Ming-Liang, Huai-Chun, and Tat-Leung (2009)]. We have imposed the boundary conditions of the stability equations by using the Chebyshev Tau method [Orszag (1971)].

In section 2 we present the physical and mathematical models of the system under analysis. Section 3 shows: (i) the base solution of the pure conductive system, (ii) the equations for the velocity and temperature perturbations of the base solution and (iii) the definition of the similarity variable η that is used to formulate the Rayleigh-Bénard problem with melting (with independent variables time t and height of the fluid layer $H(t)$) in terms of one independent variable [Kim, Lee, and Choi (2008)]. The Chebyshev Tau spectral method that we use to solve the stability equations is presented in section 4. In section 5 we present the numerical results corresponding to the critical Rayleigh number Ra_c and critical wave number a_c for different values of the rate of melting λ of the solid phase. Finally the concluding remarks are presented in section 6.

2 Mathematical model

The system under analysis is composed of a two-dimensional solid, which is semi-infinite in the horizontal dimension, sitting on a horizontal plate. A constant body force is assumed to act in the vertical direction y. At time $t > 0$, the temperature of the horizontal plate is set to a value higher than the melting temperature of the solid and a liquid layer develops between the plate, which is kept at constant temperature, and the lower part of the solid. This situation is sketched in Fig. 1. Initially, heat is transferred purely by conduction from the bottom plate to the system, subsequently melting the solid material, and given that the system is uniform in the horizontal direction x, the solid melts uniformly, hence the liquid region has a uniform height $H(t)$. As the liquid layer grows, a critical value is reached such that convective motion becomes the mechanism more stable for heat transfer.

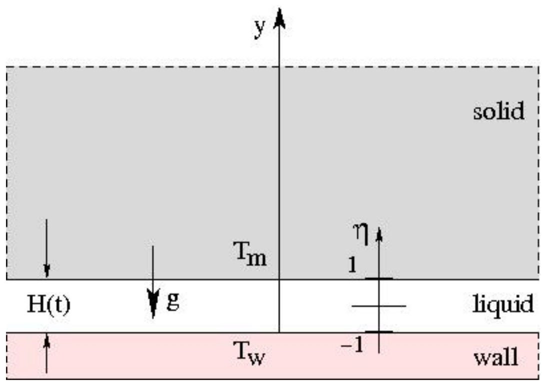

Figure 1: Sketch of the physical situation analyzed

Considering the Boussinesq approximation, the conservation equations for the liquid phase are:

$$\frac{\partial u}{\partial x}+\frac{\partial v}{\partial y}=0, \tag{1}$$

$$\frac{\partial u}{\partial t}+u\frac{\partial u}{\partial x}+v\frac{\partial u}{\partial y}=-\frac{1}{\rho_r}\frac{\partial p}{\partial x}+\nu\left(\frac{\partial^2 u}{\partial x^2}+\frac{\partial^2 u}{\partial y^2}\right), \tag{2}$$

$$\frac{\partial v}{\partial t}+u\frac{\partial v}{\partial x}+v\frac{\partial v}{\partial y}=-\frac{1}{\rho_r}\frac{\partial p}{\partial y}+\nu\left(\frac{\partial^2 v}{\partial x^2}+\frac{\partial^2 v}{\partial y^2}\right)-\frac{\rho}{\rho_r}g, \tag{3}$$

$$\frac{\partial T}{\partial t}+u\frac{\partial T}{\partial x}+v\frac{\partial T}{\partial y}=\alpha\left(\frac{\partial^2 T}{\partial x^2}+\frac{\partial^2 T}{\partial y^2}\right), \tag{4}$$

where (u,v) is the velocity vector, ρ is the density of the fluid, p is the pressure, g is the acceleration of gravity acting along the $-y$ direction, T is the temperature of the fluid and α is the thermal diffusivity of the liquid phase.
We assume that the liquid follows the state equation

$$\rho = \rho_r(1-\beta(T-T_r)) \tag{5}$$

where β is the coefficient of thermal expansion and the subindex r denotes a reference value. The boundary conditions considered are:

$$
\begin{array}{lll}
(u,v)=0 & \text{at} & \text{the bottom wall, and at } y=H(t) \\
T=T_w & \text{at} & \text{the bottom wall} \\
T=T_m & \text{at} & y=H(t) \\
-k\ \partial T/\partial y = L\ dH/dt & \text{at} & y=H(t),
\end{array}
$$

where k is the thermal conductivity of the liquid, L is the latent heat and T_m is the melting temperature.

3 Base solution

At time $t > 0$, the solid starts melting, however the fluid is motionless, i.e. u, v =0. Taking the origin of coordinates at the middle height of the fluid layer (see Fig. 1), the temperature T_o and pressure p_o in the liquid phase, for the base state, have the distributions described by [Carlslaw and Jaeger (1959)]

$$T_o = T_w - \frac{T_w - T_m}{\text{erf}\lambda}\text{erf}\left(\frac{\lambda}{2}(1+\frac{y}{2(\alpha t)^{1/2}})\right), \tag{6}$$

$$p_o = -\rho_r \int^y \left(T_w - \frac{T_w - T_m}{\text{erf}\lambda}\text{erf}\left(\frac{\lambda}{2}(1+\frac{\xi}{2(\alpha t)^{1/2}})\right)\right) d\xi, \tag{7}$$

and the liquid-solid interface recedes according to

$$H(t) = 2\lambda(\alpha t)^{1/2}. \tag{8}$$

The rate of melting λ is defined in terms of the Stefan number St by the equation

$$\pi^{1/2}\lambda e^{\lambda^2}\text{erf}(\lambda) = St, \qquad \text{where} \qquad St = \frac{Cp(T_w - T_m)}{L}. \tag{9}$$

The stability of the base solution is examined using the standard method, wherein a perturbation of the base solution is defined according to the following expressions:

$$(u,v) = (u',v'), \qquad T = T_o(y,t) + T' \qquad \text{and} \qquad p = p_o(y,t) + p'. \tag{10}$$

The equations governing the perturbations are:

$$\frac{\partial u'}{\partial x} + \frac{\partial v'}{\partial y} = 0, \tag{11}$$

$$\frac{\partial u'}{\partial t} = -\frac{1}{\rho_r}\frac{\partial p'}{\partial x} + \nu\left(\frac{\partial^2 u'}{\partial x^2} + \frac{\partial^2 u'}{\partial y^2}\right), \tag{12}$$

$$\frac{\partial v'}{\partial t} = -\frac{1}{\rho_r}\frac{\partial p'}{\partial y} + \nu\left(\frac{\partial^2 v'}{\partial x^2} + \frac{\partial^2 v'}{\partial y^2}\right) - g\beta T', \tag{13}$$

and

$$\frac{\partial T'}{\partial t} + v'\frac{\partial T_o}{\partial y} = \alpha\left(\frac{\partial^2 T'}{\partial x^2} + \frac{\partial^2 T'}{\partial y^2}\right). \tag{14}$$

The pressure perturbation is eliminated using Eqs. (12) and (13) to get

$$\frac{\partial \nabla^2 v'}{\partial t} = \nu\nabla^4 v' - g\beta\frac{\partial^2 T'}{\partial x^2}, \tag{15}$$

and the equation for the temperature perturbation is

$$\frac{\partial T'}{\partial t} + v'\frac{\partial T_o}{\partial y} = \alpha\nabla^2 T' \tag{16}$$

At this point, it is convenient to define the variables

$$\eta = \frac{2y}{H}, \qquad v^* = \frac{H}{2\alpha}v' \qquad \text{and} \qquad T^* = \frac{\beta g H^3}{8\alpha\nu}T', \tag{17}$$

Notice that η is the similarity variable, and if the origin is located at the middle height of the fluid layer, η is in the range $-1 \leq \eta \leq 1$.
In terms of η, v^* and T^*, Eqs. (15) and (16) can be written as

$$-\frac{1}{t}\frac{\partial^2 v^*}{\partial x^2}-\frac{\eta}{t}\frac{\partial^2}{\partial x^2}\frac{\partial v^*}{\partial \eta}-\frac{12}{H^2 t}\frac{\partial^2 v^*}{\partial \eta^2}-\frac{4\eta}{H^2 t}\frac{\partial^3 v^*}{\partial \eta^3}= \\ 4\nu\left(H^2\frac{\partial^4 v^*}{\partial x^4}+4\frac{\partial^2}{\partial x^2}\frac{\partial^2 v^*}{\partial \eta^2}+\frac{16}{H^2}\frac{\partial^4 v^*}{\partial \eta^4}\right)-\frac{2\nu}{\alpha}\left(\frac{\partial^2 T^*}{\partial x^2}\right) \tag{18}$$

and

$$\frac{\partial T^*}{\partial t}-\frac{3T^*}{t}-\alpha\left(\frac{\partial^2 T^*}{\partial x^2}+\frac{4}{H^2}\frac{\partial^2 T^*}{\partial \eta^2}\right)=-\frac{g\beta}{H}v^*\frac{\partial T_o}{\partial \eta} \tag{19}$$

We now proceed with the standard modal analysis along the x direction by defining F_u and F_T as:

$$v^* = F_v(\eta)e^{ikx} \qquad \text{and} \qquad T^* = F_T(\eta)e^{ikx}. \tag{20}$$

Upon substituting the previous expressions in equation (18), we get

$$\left(4\frac{d^2}{d\eta^2}-a^2\right)^2 F_v-\frac{2a^2\eta}{\tau Pr}\frac{dF_v}{d\eta}+\frac{8\eta}{\tau Pr}\frac{d^3F_v}{d\eta^3}-\frac{2a^2}{\tau Pr}F_v+ \\ \frac{24}{\tau Pr}\frac{d^2F_v}{d\eta^2}+4a^2F_T=0, \tag{21}$$

where $a = kH$ is the wave number, $\tau = 4\alpha t/H^2$ is the scaled time and $Pr = \nu/\alpha$ is the Prandtl number. Following a similar procedure, Eq. (19) may be written as

$$4\frac{d^2F_T}{d\eta^2}+\frac{2\eta}{\tau}\frac{dF_T}{d\eta}-\frac{1}{\tau}\left(\tau a^2-6\right)F_T=\frac{1}{2}RaF_v\frac{d\bar{T}_o}{d\eta}, \tag{22}$$

where the Rayleigh number Ra is defined as

$$Ra=\frac{\beta g\left(T_w-T_m\right)H^3(t)}{\nu\alpha}, \tag{23}$$

and the scaled base temperature is $\bar{T}_o = (T_o - T_w)/(T_w - T_m)$.

Six boundary conditions are required to solve Eqs. (21) and (22). The following four boundary conditions indicate that the perturbations vanish at the horizontal boundaries [Bourne (2003)], hence

$$F_v(\eta=-1)=F_T(\eta=-1)=F_v(\eta=1)=F_T(\eta=1)=0. \tag{24}$$

Two additional boundary conditions are used to define the kind of surface in contact with the fluid. In the case of a rigid lower hot surface and a rigid interface, we have

$$DF_v(\eta=-1)=DF_v(\eta=1)=0. \tag{25}$$

The last boundary condition $DF_T(\eta=1)=0$ has been introduced since it is assumed that at the interface ($\eta=1$) the heat flux, towards the solid phase due to the perturbation of the temperature F_T, is equal to zero. This assumption is valid because the temperature of the solid phase at $\eta\to\infty$ is equal to the melting temperature and hence, there is no heat transfer in the solid phase.

4 Numerical method

We use expansions in Chebyshev polynomials to approximate the solution to Eqs. (21) and (22) and boundary conditions Eqs. (24) and (25). It is possible to expand the variables $F_v(\eta)$ and $F_T(\eta)$ in the interval $-1\le\eta\le1$ as:

$$F_v(\eta)=\sum_{n=0}^{\infty}a_{vn}T_n(\eta), \qquad F_T(\eta)=\sum_{n=0}^{\infty}a_{Tn}T_n(\eta) \tag{26}$$

where $T_n(\eta)$ are the nth-degree Chebyshev polynomials of the first kind, which satisfy the orthogonality relation [Orszag (1971); Dongarra, Straughan, and Walker (1996)]

$$\int_{-1}^{1}T_n(\eta)\,T_m(\eta)\left(1-\eta^2\right)^{-1/2}d\eta=\frac{\pi}{2}c_n\delta_{nm} \tag{27}$$

where $c_0=2$, $c_n=1$ for $n>0$.

In the numerical procedure we seek an approximate solution of the equations of the form

$$F_v(\eta)=\sum_{n=0}^{N}a_{vn}T_n(\eta), \qquad F_T(\eta)=\sum_{n=0}^{N}a_{Tn}T_n(\eta). \tag{28}$$

Equations for the expansion coefficients a_{vn} and a_{Tn} are generated by substituting Eq. (28) into Eqs. (21) and (22), and applying the orthogonality property (27). It is possible to find in the published literature explicit formulae to relate the expansion coefficients a_n in the series

$$f(\eta) = \sum_{n=0}^{N} a_n T_n(\eta), \tag{29}$$

to the expansion coefficients b_n of various linear operators $\hat{L}$ represented as

$$\hat{L}f(\eta) = \sum_{n=0}^{N} b_n T_n(\eta). \tag{30}$$

Specifically, expressions for the following operators: $\hat{L}f(\eta) = d^4 f(\eta)/d\eta^4$, $\hat{L}f(\eta) = d^2 f(\eta)/d\eta^2$ and $\hat{L}f(\eta) = \eta df(\eta)/d\eta$, in terms of Chebyshev polynomials are available in references [Orszag (1971)] or [Gottlieb and Orszag (1977)]. However, the corresponding expressions for the operators: $\hat{L}f(\eta) = \eta d^3 f(\eta)/d\eta^3$ and

$$\hat{L}f(\eta) = \eta^m F_v(\eta) = \eta^m \left(\sum_{n=0}^{N} a_{vn} T_n(\eta) \right), \tag{31}$$

(see Eqs. (43) and (51) below), are not available in the literature, so they were generated through a computational procedure in which the polynomials $T_n(\eta)$ (or their derivatives) in Eq. (31) are represented by the recursive relation

$$T_0(\eta) = 1, \qquad T_1(\eta) = \eta \tag{32}$$

and

$$T_{n+1}(\eta) = 2\eta T_n(\eta) - T_{n-1}(\eta), \qquad \text{for } n \geq 1 \tag{33}$$

and then, the term η^m of Eq. (31) is expanded using the following expression in terms of the Chebyshev polynomials [Thacher (1964)]:

$$\eta^m = \sum_{q=0}^{m} \Theta_{m,q} T_q(\eta) \tag{34}$$

where

$$\Theta_{m,q} = \begin{cases} 2^{1-m} \binom{m}{\frac{m-q}{2}} & m-q \ \text{ even} \\ 0 & m-q \ \text{ odd,} \end{cases} \tag{35}$$

In the summation of Eq. (34), it must be considered that the first term is to be divided by two. After these substitutions, the coefficients of the Chebyshev polynomials $T_n(\eta)$, see Eq. (34), are the coefficients b_n of the operator

$$\hat{L}f(\eta) = \eta^m F_v(\eta) = \sum_{n=0}^{N} b_n T_n(\eta)\,. \tag{36}$$

The derivative of $\bar{T}_o$ with respect the similarity variable η, which is used in the perturbation equation for the temperature, see Eq. (22), has been evaluated following two methodologies. In the first procedure, the function $\mathrm{erf}(0.5\lambda\,(1+\eta))$ is approximated using its Taylor expansion of ninth degree

$$\mathrm{erf}\Big(0.5\lambda\,(1+\eta)\Big) = \frac{2}{\pi^{1/2}}\Big\{0.5\lambda\,(1+\eta) - \frac{1}{3}\left(0.5\lambda\,(1+\eta)\right)^3 + \tag{37}$$
$$\frac{1}{10}\left(0.5\lambda\,(1+\eta)\right)^5 - \frac{1}{42}\left(0.5\lambda\,(1+\eta)\right)^7 + \frac{1}{216}\left(0.5\lambda\,(1+\eta)\right)^9\Big\},$$

then, the derivative of Eq. (37) is

$$\frac{d}{d\eta}\Big(\mathrm{erf}\Big(0.5\lambda\,(1+\eta)\Big)\Big) = \frac{\lambda}{\pi^{1/2}}\Big\{1 - \left(\frac{\lambda}{2}(1+\eta)\right)^2 + \frac{5}{10}\left(\frac{\lambda}{2}(1+\eta)\right)^4 - \tag{38}$$
$$\frac{7}{42}\left(\frac{\lambda}{2}(1+\eta)\right)^6 + \frac{9}{216}\left(\frac{\lambda}{2}(1+\eta)\right)^8\Big\}.$$

Each term in Eq. (38), is expanded to have the following expressions:

$$\left(\frac{\lambda}{2}(1+\eta)\right)^2 = \frac{\lambda^2}{4}\left(1+2\eta+\eta^2\right), \tag{39}$$

$$\left(\frac{\lambda}{2}(1+\eta)\right)^4 = \frac{\lambda^4}{16}\left(1+4\eta+6\eta^2+4\eta^3+\eta^4\right), \tag{40}$$

$$\left(\frac{\lambda}{2}(1+\eta)\right)^6 = \frac{\lambda^6}{64}\left(1+6\eta+15\eta^2+20\eta^3+15\eta^4+6\eta^5+\eta^6\right) \tag{41}$$

and

$$\left(\frac{\lambda}{2}(1+\eta)\right)^8 = \frac{\lambda^8}{256}\left(1+8\eta+28\eta^2+56\eta^3+70\eta^4+56\eta^5+28\eta^6+8\eta^7+\eta^8\right).$$

(42)

Consequently, the term on the right hand side of Eq. (22) may be written as

$$\frac{1}{2}RaF_v\frac{d\bar{T}_o}{d\eta} = -\frac{1}{2}RaF_v\frac{1}{\mathrm{erf}(\lambda)}\frac{\lambda}{\pi^{1/2}}\left\{1-\frac{\lambda^2}{4}\left(1+2\eta+\eta^2\right)+\right. \quad (43)$$
$$\frac{5\lambda^4}{160}\left(1+4\eta+6\eta^2+4\eta^3+\eta^4\right)-$$
$$\frac{7\lambda^6}{2688}\left(1+6\eta+15\eta^2+20\eta^3+15\eta^4+6\eta^5+\eta^6\right)+$$
$$\left.\frac{9\lambda^8}{55296}\left(1+8\eta+28\eta^2+56\eta^3+70\eta^4+56\eta^5+28\eta^6+8\eta^7+\eta^8\right)\right\}.$$

In the second procedure, the derivative of the error function $\mathrm{erf}(0.5\lambda\,(1+\eta))$ was evaluated as

$$\frac{d}{d\eta}\left(\mathrm{erf}\left(0.5\lambda\,(1+\eta)\right)\right) = \frac{\lambda}{\pi^{1/2}}\exp-\left(\frac{\lambda}{2}(1+\eta)\right)^2. \quad (44)$$

The Chebyshev approximation polynomial $P_N(\eta)$ of degree $\leq N$ for a function $f(\eta)$ over $[-1,1]$ can be written as a sum of Chebyshev polynomials $T_j(\eta)$ [Mathews and Fink (2004)]

$$f(\eta) \approx P_N(\eta) = \sum_{j=0}^{N} c_j T_j(\eta). \quad (45)$$

The coefficients c_j are computed with the formulae

$$c_0 = \frac{1}{N+1}\sum_{k=0}^{N} f(\eta_k)\,T_0(\eta_k) = \frac{1}{N+1}\sum_{k=0}^{N} f(\eta_k) \quad (46)$$

and

$$c_j = \frac{2}{N+1}\sum_{k=0}^{N} f(\eta_k)\,T_j(\eta_k) \quad (47)$$

or

$$c_j = \frac{2}{N+1}\sum_{k=0}^{N} f(\eta_k)\cos\left(\frac{j\pi(2k+1)}{2N+2}\right) \text{ for} j = 1,2,....N. \quad (48)$$

The nodes η_k are evaluated as

$$\eta_k = \cos\left(\pi\frac{2k+1}{2N+2}\right) \qquad \text{for} \qquad k = 0,1,...N. \quad (49)$$

In this investigation, we used N =30. Once the coefficients c_j of the Chebyshev approximation polynomial $P_N(\eta)$ of the function $\exp-(0.5\lambda(1+\eta))^2$ have been determined, see Eq. (45), i.e.

$$\exp-\left(\frac{\lambda}{2}(1+\eta)\right)^2 = c_0T_0(\eta)+c_1T_1(\eta)+.....c_{30}T_{30}, \tag{50}$$

the Chebyshev polynomials $T_j(\eta)$ of Eq. (50), were written in terms of the variable η, see Eqs. (32) and (33). Therefore the term on the right hand side of Eq. (22), can also be written as

$$\frac{1}{2}RaF_v\frac{d\Theta}{d\eta} = -\frac{1}{2}RaF_v\frac{1}{\text{erf}(\lambda)}\frac{\lambda}{\pi^{1/2}}\exp-\left(\frac{\lambda}{2}(1+\eta)\right)^2 = \tag{51}$$
$$-\frac{1}{2}RaF_v\frac{1}{\text{erf}(\lambda)}\frac{\lambda}{\pi^{1/2}}\Big(c_0(1)+c_1\eta+c_2\left(2\eta^2-1\right)+c_3\left(4\eta^3-3\eta\right)+$$
$$c_4\left(8\eta^4-8\eta^2+1\right)+c_5\left(16\eta^5-20\eta^3+5\eta\right)+...\Big).$$

The method that we have selected to obtain the equations for the coefficients a_{vn} and a_{Tn} is the Chebyshev Tau method, which has been extensively used to solve ordinary differential equations, such as the linear hydrodynamic and thermal instability equations. The main idea of the Chebyshev Tau method is to generate (by substituting the expansions (28) into Eqs. (21) and (22)), one equation for each $n = 0,1,2....2N-6$. The remaining seven equations, those for $2N-5 \leq n \leq 2N+1$ are generated by using the six boundary conditions Eqs. (24) and (25) and the condition at the interface $DF_T(\eta = 1) = 0$. The high frequency behaviour (i.e. high n) of the solution is not governed by the dynamical and thermal Eqs. (21) and (22), but by the boundary conditions [Orszag (1971)]. The Tau equations can be written as a generalized eigenvalue problem (**Ax**)= Ra (**Bx**), where the vector **x** includes the coefficients a_{vn} and a_{Tn}, Ra is the Rayleigh number, and **A** and **B** are $(2(N+1))\times(2(N+1))$ matrices whose first $2(N+1)-7$ rows are defined by Eqs. (21) and (22). The last seven rows of **A** are given by the boundary conditions, and the last seven rows of **B** vanish [McFadden, Murray, and Boisvert (1990)]. A schematic representation of the matrix equations for the case $N = 8$ is,

$$
\mathbf{A}=\left|\begin{array}{cccccccccccccccccc}
x & 0 & x & 0 & x & 0 & x & 0 & x & x & 0 & 0 & 0 & 0 & 0 & 0 & 0 & 0 \\
0 & x & 0 & x & 0 & x & 0 & x & 0 & 0 & x & 0 & 0 & 0 & 0 & 0 & 0 & 0 \\
0 & 0 & x & 0 & x & 0 & x & 0 & x & 0 & 0 & x & 0 & 0 & 0 & 0 & 0 & 0 \\
0 & 0 & 0 & x & 0 & x & 0 & x & 0 & 0 & 0 & 0 & x & 0 & 0 & 0 & 0 & 0 \\
0 & 0 & 0 & 0 & x & 0 & x & 0 & x & 0 & 0 & 0 & 0 & x & 0 & 0 & 0 & 0 \\
0 & 0 & 0 & 0 & 0 & x & 0 & x & 0 & 0 & 0 & 0 & 0 & 0 & x & 0 & 0 & 0 \\
0 & 0 & 0 & 0 & 0 & 0 & x & 0 & x & 0 & 0 & 0 & 0 & 0 & 0 & x & 0 & 0 \\
0 & 0 & 0 & 0 & 0 & 0 & 0 & x & 0 & 0 & 0 & 0 & 0 & 0 & 0 & 0 & x & 0 \\
0 & 0 & 0 & 0 & 0 & 0 & 0 & 0 & x & 0 & 0 & 0 & 0 & 0 & 0 & 0 & 0 & x \\
0 & 0 & 0 & 0 & 0 & 0 & 0 & 0 & 0 & x & 0 & x & 0 & x & 0 & x & 0 & x \\
0 & 0 & 0 & 0 & 0 & 0 & 0 & 0 & 0 & 0 & x & 0 & x & 0 & x & 0 & x & 0 \\
x & x & x & x & x & x & x & x & x & 0 & 0 & 0 & 0 & 0 & 0 & 0 & 0 & 0 \\
x & x & x & x & x & x & x & x & x & 0 & 0 & 0 & 0 & 0 & 0 & 0 & 0 & 0 \\
0 & x & x & x & x & x & x & x & x & 0 & 0 & 0 & 0 & 0 & 0 & 0 & 0 & 0 \\
0 & x & x & x & x & x & x & x & x & 0 & 0 & 0 & 0 & 0 & 0 & 0 & 0 & 0 \\
0 & 0 & 0 & 0 & 0 & 0 & 0 & 0 & 0 & x & x & x & x & x & x & x & x & x \\
0 & 0 & 0 & 0 & 0 & 0 & 0 & 0 & 0 & x & x & x & x & x & x & x & x & x \\
0 & 0 & 0 & 0 & 0 & 0 & 0 & 0 & 0 & x & x & x & x & x & x & x & x & x
\end{array}\right|
$$

and

$$
\mathbf{B}=\left|\begin{array}{cccccccccccccccccc}
0 & 0 & 0 & 0 & 0 & 0 & 0 & 0 & 0 & 0 & 0 & 0 & 0 & 0 & 0 & 0 & 0 & 0 \\
0 & 0 & 0 & 0 & 0 & 0 & 0 & 0 & 0 & 0 & 0 & 0 & 0 & 0 & 0 & 0 & 0 & 0 \\
0 & 0 & 0 & 0 & 0 & 0 & 0 & 0 & 0 & 0 & 0 & 0 & 0 & 0 & 0 & 0 & 0 & 0 \\
0 & 0 & 0 & 0 & 0 & 0 & 0 & 0 & 0 & 0 & 0 & 0 & 0 & 0 & 0 & 0 & 0 & 0 \\
0 & 0 & 0 & 0 & 0 & 0 & 0 & 0 & 0 & 0 & 0 & 0 & 0 & 0 & 0 & 0 & 0 & 0 \\
0 & 0 & 0 & 0 & 0 & 0 & 0 & 0 & 0 & 0 & 0 & 0 & 0 & 0 & 0 & 0 & 0 & 0 \\
0 & 0 & 0 & 0 & 0 & 0 & 0 & 0 & 0 & 0 & 0 & 0 & 0 & 0 & 0 & 0 & 0 & 0 \\
0 & 0 & 0 & 0 & 0 & 0 & 0 & 0 & 0 & 0 & 0 & 0 & 0 & 0 & 0 & 0 & 0 & 0 \\
0 & 0 & 0 & 0 & 0 & 0 & 0 & 0 & 0 & 0 & 0 & 0 & 0 & 0 & 0 & 0 & 0 & 0 \\
x & x & x & x & x & x & x & x & x & 0 & 0 & 0 & 0 & 0 & 0 & 0 & 0 & 0 \\
x & x & x & x & x & x & x & x & x & 0 & 0 & 0 & 0 & 0 & 0 & 0 & 0 & 0 \\
0 & 0 & 0 & 0 & 0 & 0 & 0 & 0 & 0 & 0 & 0 & 0 & 0 & 0 & 0 & 0 & 0 & 0 \\
0 & 0 & 0 & 0 & 0 & 0 & 0 & 0 & 0 & 0 & 0 & 0 & 0 & 0 & 0 & 0 & 0 & 0 \\
0 & 0 & 0 & 0 & 0 & 0 & 0 & 0 & 0 & 0 & 0 & 0 & 0 & 0 & 0 & 0 & 0 & 0 \\
0 & 0 & 0 & 0 & 0 & 0 & 0 & 0 & 0 & 0 & 0 & 0 & 0 & 0 & 0 & 0 & 0 & 0 \\
0 & 0 & 0 & 0 & 0 & 0 & 0 & 0 & 0 & 0 & 0 & 0 & 0 & 0 & 0 & 0 & 0 & 0 \\
0 & 0 & 0 & 0 & 0 & 0 & 0 & 0 & 0 & 0 & 0 & 0 & 0 & 0 & 0 & 0 & 0 & 0 \\
0 & 0 & 0 & 0 & 0 & 0 & 0 & 0 & 0 & 0 & 0 & 0 & 0 & 0 & 0 & 0 & 0 & 0
\end{array}\right|
$$

The vector of unknown coefficients **x** is,

$$\mathbf{x}^T = \begin{bmatrix} a_{v0} & a_{v1} & a_{v2} & a_{v3} & a_{v4} & a_{v5} & a_{v6} & a_{v7} & a_{v8} & a_{T0} & a_{T1} & a_{T2} & a_{T3} & a_{T4} & a_{T5} & a_{T6} & a_{T7} & a_{T8} \end{bmatrix}^T.$$

In the matrices **A** and **B** the non-zero entries are denoted by x. The system of equations has been solved numerically by using the routine F02GJF from the NAG library. The routine F02GJF calculates all the eigenvalues of the eigenproblem **A x**= $\hat{\lambda}$ **B x**, by using the QZ algorithm (see http://www.nag.co.uk/numeric/Fl/manual/xhtml/F02/f02gjf.xml).

5 Results

In this section we present examples of the critical Rayleigh numbers and wave numbers corresponding to the solutions to Eqs. (21) and (22), obtained with the numerical method described in Section 4. We have found that the critical Rayleigh and wave numbers strongly depend on the rate of melting λ. For water at atmospheric pressure, the Stefan number is in the range $0.06 \leq St \leq 1$, when the temperature varies between 5^oC and 80^oC, whereas the rate of melting λ in the same range of temperatures varies from $\lambda \approx 0.1$ to $\lambda \approx 0.6$. For metals $\lambda \sim 1$, therefore we will focus the analysis in this range of λ. Note also that if no phase change takes place, then $\lambda = 0$ and the analysis should reduce to that of the classical Rayleigh-Bénard problem. Fig. 2 shows the Rayleigh numbers Ra at which the instability sets in as a function of the wave number a for $\lambda = 0.1$ and $Pr = 10$. The various curves correspond to the four least stable eigenvalues (Ra numbers) evaluated by the Chebyshev Tau spectral method. The most unstable eigenvalue, Ra_c, is found to be 1702.3566 at a_c equal to 3.112. The effect of increasing the parameter λ can be observed in Fig. 3. As it can be appreciated, both the critical Rayleigh number and the critical wave number are reduced, as λ increases. Fig. 4 shows the same results as the previous graphs, but for λ= 1.411. It was found that for $\lambda > 1.411$, the base solution is always unstable. Note from Figs. (2) to (4) that the other three least stable eigenvalues are independent on the rate of melting λ. A remark should be given at this point, the second least stable eigenvalue (second curve from bottom to top in Figs. (2) to (4)) is very similar to the curve shown by [Chandrasekhar (1961)], see page 39 -notice that in Chandrasekhar's book the scale for the first odd (curve labelled 2) mode is missing- however the values shown in page 38 of that book, are in agreement with the values obtained by the Chebyshev Tau spectral method. Whereas Chandrasekhar obtained for the first odd mode, Ra=17610.39 and a=5.365, we calculated for the second least stable eigenvalue, Ra=17537.465 and a=5.355. It seems that the least stable eigenvalues (except the most unstable, Ra_c) in a melting process from below, are governed by thermo-physical phenomena similar to those present in the classical Rayleigh-Bénard problem.

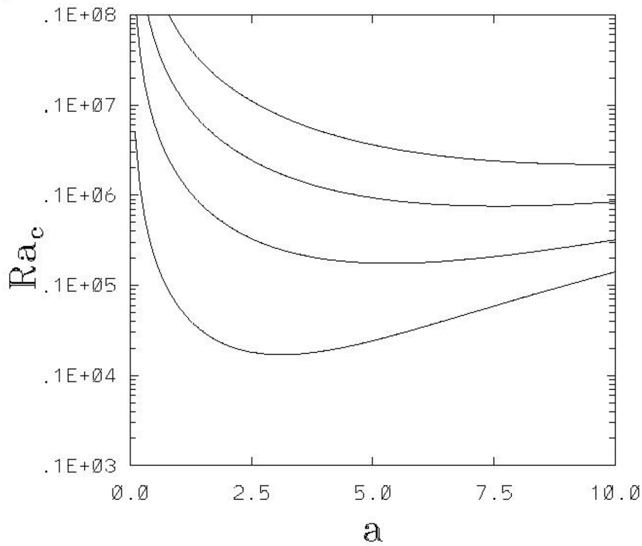

Figure 2: Rayleigh number *Ra* as a function of wave number a for $\lambda = 0.1$ and $Pr = 10$. The most unstable critical Rayleigh number is $Ra_c = 1702.3566$ and the corresponding critical wave number is $a_c = 3.1120$. Chebyshev Polynomial degree $N = 30$.

Figure 5 shows the general trend of Ra_c and a_c as functions of λ. In the limit when $\lambda \to 0$, $Ra_c \to 1708$ and $a_c \to 3.1$, the classical Rayleigh-Bénard solution is recovered. All examples presented above were obtained for *Pr*=10, and further numerical calculations indicate that the results are essentially the same for Prandtl numbers up to 10,000, with slightly higher Ra_c for the larger values of the Prandtl number. For instance for *Pr*=10,000, we obtain the following set of values: (i) λ=0.1, Ra_c=1702.44, and a_c=3.112; (ii) $\lambda = 1$, Ra_c=1211.842 and a_c=2.748; (iii) $\lambda = 1.411$, Ra_c=552.72 and a_c=0.956.

Numerical calculations were also carried out to obtain the critical values for low Prandtl number fluid layers, *Pr*=0.0l. The obtained results indicate that Ra_c and a_c are nonmonotonic functions of the parameter λ. A similar behaviour, but for the quasi-static case, was reported by [Sparrow, Lee, and Shamsundar (1976)]. They concluded that the variation of the motionless base state temperature profile as the Stefan number (the parameter λ) is modified, leads to a nonmonotonic behaviour of the critical Rayleigh number. Further research will be performed by the authors of the present investigation in order to identify the physical and thermal characteristics of the system that conduct to the presence of an extremum value of the critical

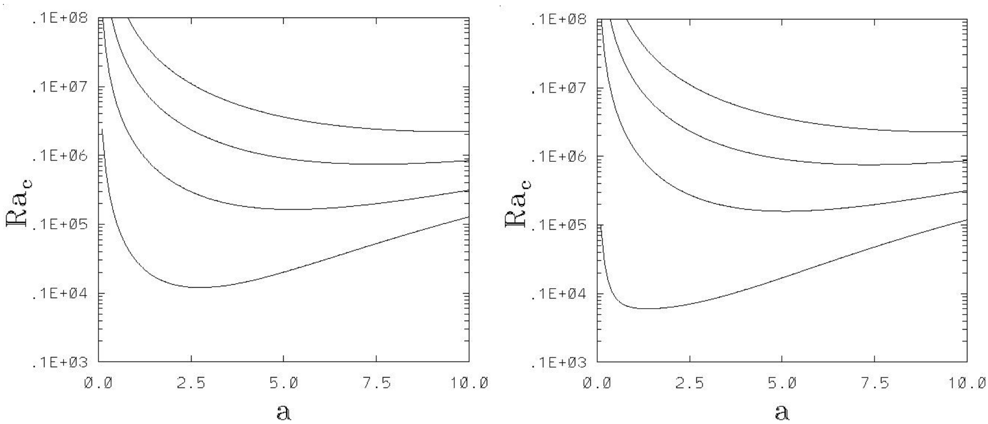

Figure 3: Rayleigh number Ra as a function of wave number a for $Pr = 10$. $\lambda = 1.0$ in the left panel and $\lambda = 1.4$ in the right panel. The critical Rayleigh and wave numbers are $Ra_c = 1204.7583$, $a_c = 2.74$ and $Ra_c = 599.7701$, $a_c = 1.348$ respectively. Chebyshev Polynomial degree $N = 30$.

parameters. We obtain the following set of values for the case with Pr=0.01: (i) λ=0.1, Ra_c=1610.401, and a_c=3.076; (ii) $\lambda = 0.5$, Ra_c=273.977, and a_c=1.7632; (iii) $\lambda = 1$, Ra_c=135.671, and a_c=1.751; (iv) $\lambda = 1.2$, Ra_c=409.32, and a_c=3.017; (v) $\lambda = 1.411$, Ra_c=1151.7091, and a_c=4.33199. Note that as the parameter $\lambda \to 0$, the Rayleigh-Bénard solution is recovered. On the other hand, it is observed that both critical parameters at first decrease, reach a minimum and then increase.

6 Conclusions

We developed a robust numerical method to solve the set of differential equations that describe the stability of a two dimensional fluid layer confined between a horizontal rigid wall and a melting upper surface. We found that the critical Rayleigh and wave numbers are monotonically decreasing functions of the receding velocity of the front. The parameters Ra_c and a_c are independent functions of the Pr number in the range $1 \leq Pr \leq 10,000$. The second, third and fourth least stable eigenvalues are also independent functions of the Pr number and the parameter λ. We have found that the second least stable eigenvalue resembles the first odd mode of the classical Rayleigh-Bénard problem. We have shown that the critical parameters present a nonmonotonic variation with the melting rate λ for low Prandtl number fluid layers (Pr=0.01). Extensions to the analysis presented here that can be solved

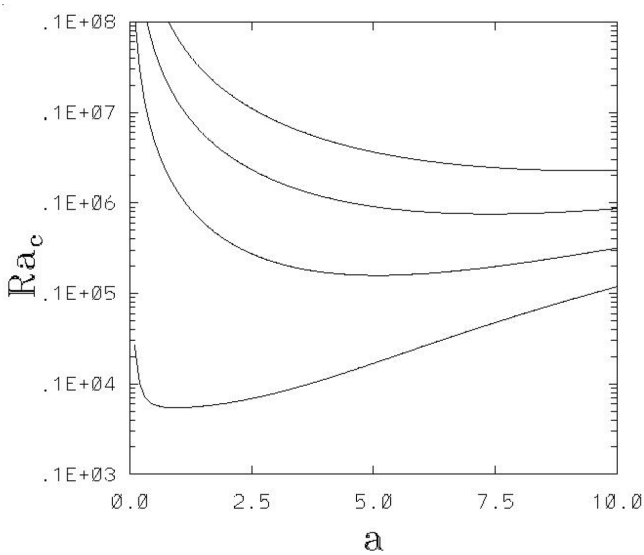

Figure 4: Rayleigh number Ra as a function of wave number a for $\lambda = 1.411$ and $Pr = 10$. Critical Rayleigh number $Ra_c = 544.9554$ and critical wave number $a_c = 0.956$. Chebyshev Polynomial degree $N = 30$.

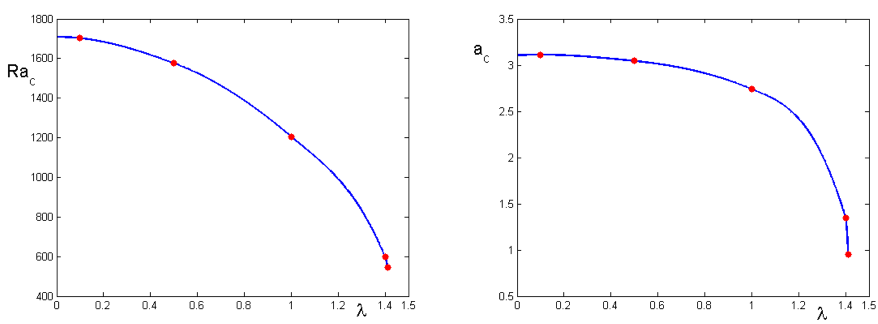

Figure 5: Critical Rayleigh number Ra_c and wave number a_c as a functions of λ. The dots are actual calculations, and the lines are interpolations with piecewise cubic Hermite polynomials. In all cases, Chebyshev Polynomial degree $N = 30$.

with simple modifications to our numerical method include the study of the stability of a three dimensional slab of liquid with infinite horizontal extensions. Also, the consideration of a temperature different from the melting temperature at a finite distance from the melting front can be analyzed using the numerical method presented here. Few experimental realizations of the system analyzed here are available in the literature, see for instance [Yen (1968)], but a direct comparison might be difficult, mainly due to the possibility that the instability triggered by the bounding vertical walls of the experimental device, manifests itself before the convective instability which has been described in this investigation.

Acknowledgment: Financial support for this investigation was provided by DGAPA-UNAM (sabbatical leave of R. Avila at the Center for Aerospace Research & Education, University of California, Irvine) and DGSCA-UNAM through the Visualization Observatory (Ixtli project). Most of the computations were carried out on the supercomputer of DGSCA-UNAM and on the Linux-based 'BDUC' cluster at the University of California, Irvine.

References

Asmolov, V.; Ponomarev-Stepnoy, N. N.; Strizhov, V.; Sehgal, B. R. (2001): Challenges left in the area of in-vessel melt retention. *Nuclear Engineering and Design*, vol. 209, pp. 87–96.

Atluri, S. N.; Zhu, T. (1998): A new Meshless Local Petrov-Galerkin (MLPG) approach in computational mechanics. *Computational Mechanics*, vol. 22, pp. 117–127.

Avila, R.; Solorio, F. J. (2009): Numerical solution of 2D natural convection in a concentric annulus with solid-liquid phase change. *CMES: Computer Modeling in Engineering & Sciences*, vol. 44, pp. 177–202.

Boger, D. V.; Westwater, J. W. (1967): Effect of buoyancy on the melting and freezing process. *Journal of Heat Transfer, Transactions of ASME*, vol. 89, pp. 81–89.

Bourne, D. (2003): Hydrodynamic stability, the Chebyshev tau method and spurious eigenvalues. *Cont. Mech. Thermodynamics*, vol. 15, pp. 571–579.

Carlslaw, H. S.; Jaeger, J. C. (1959): *Conduction of heat in solids*. Clarendon, Oxford.

Chandrasekhar, S. (1961): *Hydrodynamic and hydromagnetic stability*. Clarendon, Oxford.

Dongarra, J. J.; Straughan, B.; Walker, D. W. (1996): Chebyshev tau-QZ algorithm methods for calculating spectra of hydrodynamic stability problems. *Appl. Num. Mathematics*, vol. 22, pp. 399–434.

Getling, A. V. (1998): *Rayleigh-Bénard convection; Structures and Dynamics*. World Scientific.

Gottlieb, D.; Orszag, S. A. (1977): Numerical analysis of spectral methods: Theory and applications. In *CBMS-NSF Regional Conference Series in Applied Mathematics, Vol. 26*. SIAM, Philadelphia.

Hwang, I. G. (2001): Convective instability in porous media during solidification. *AIChE J.*, vol. 2001, pp. 1698–1700.

Kim, M. C.; Lee, D. W.; Choi, C. K. (2008): Onset of buoyancy-driven convection in melting from below . *Korean J. Chem. Eng.*, vol. 25, pp. 1239–1244.

Koschmieder, E. L. (1993): *Benard cells and Taylor vortices*. Cambridge University Press.

Kosec, G.; Šarler, B. (2009): Solution of phase change problems by collocation with local pressure correction. *CMES: Computer Modeling in Engineering & Sciences*, vol. 47, pp. 191–216.

Langlois, W. E. (1985): Buoyancy-Driven Flows in Crystal-Growth Melts. *Ann. Rev. Fluid Mech.*, vol. 17, pp. 191–215.

Lin, H.; Atluri, S. N. (2001): The Meshless Local Petrov-Galerkin (MLPG) method for solving incompressible Navier-Stokes equations. *CMES: Computer Modeling in Engineering & Sciences*, vol. 2, pp. 117–142.

Liu, C.-S. (2006): Efficient shooting methods for the second-order ordinary differential equations. *CMES: Computer Modeling in Engineering & Sciences*, vol. 15, pp. 69–86.

Liu, C.-S. (2008): A Lie-Group Shooting method for computing eigenvalues and eigenfunctions of Sturm-Liouville problems. *CMES: Computer Modeling in Engineering & Sciences*, vol. 26, pp. 157–168.

Liu, C.-S.; Chang, C.-W.; Chang, J.-R. (2008): A new shooting method for solving boundary layer equations in fluid mechanics. *CMES: Computer Modeling in Engineering & Sciences*, vol. 32, pp. 1–15.

Mathews, J. H.; Fink, K. K. (2004): *Numerical methods using Matlab*. Prentice-Hall Inc.

McFadden, G. B.; Murray, B. T.; Boisvert, R. F. (1990): Elimination of spurious eigenvalues in the Chebyshev tau spectral method. *J. Comp. Physics*, vol. 91, pp. 228–239.

Ming-Liang, X.; Huai-Chun, Z.; Tat-Leung, C. (2009): An improved Petrov-Galerkin spectral collocation solution for linear stability of circular jet. *CMES: Computer Modeling in Engineering & Sciences*, vol. 46, pp. 271–289.

Orszag, A. S. (1971): Accurate solution of the Orr-Sommerfeld stability equation. *J. Fluid Mech.*, vol. 50, pp. 689–703.

Rayleigh, L. (1916): On convection currents in horizontal layer of fluid when the higher temperature is on the under side. *Philos. Mag. Ser. 6*, vol. 32, pp. 529–546.

Ribe, N. M. (1985): The generation and composition of partial melts in the earth's mantle. *Earth and Planetary Science Letters*, vol. 73, pp. 361–376.

Smith, M. K. (1988): Thermal convection during the directional solidification of a pure liquid with variable viscosity. *J. Fluid Mech.*, vol. 188, pp. 547–570.

Sparrow, E. M.; Lee, L.; Shamsundar, N. (1976): Convective instability in a melt layer heated from below. *ASME Journal of Heat Transfer*, vol. 98, pp. 88–94.

Sparrow, E. M.; Schmidt, S. S.; Ramsey, J. W. (1978): Experiments on the role of natural convection in the melting of solids. *Journal of Heat Transfer, Transactions of ASME*, vol. 100, pp. 11–16.

Stefan, J. (1891): Ueber die theorie der eisbildung insbesondere uber die eisbildung im polarmeere. *Annalen der Physik und Chemie*, vol. 42, pp. 269–286.

Thacher, H. C. (1964): Conversion of a power to a series of Chebyshev polynomials. *Communications of the ACM*, vol. 7, pp. 181–182.

Yen, Y. C. (1968): Onset of convection in a layer of water formed by melting ice from below. *Phys. Fluids*, vol. 11, pp. 1263–1270.

Zhang, Y.; Su, Y.; Zhu, Y.; Hu, X. (2001): A General model for analyzing the thermal performance of the heat charging and discharging processes of latent heat thermal energy storage systems. *ASME J. Sol. Energy Eng.*, vol. 123, pp. 232–236.